Participation of H^+ in the Ca^{2+}-Induced Conformational Transition of 4-Nitro-2,1,3-benzoxadiazole-Labeled Sarcoplasmic Reticulum ATPase†

Shigeo Wakabayashi, Tarou Ogurusu, and Munekazu Shigekawa*

Department of Molecular Physiology, National Cardiovascular Center Research Institute, Suita, Osaka 565, Japan

Received June 1, 1990; Revised Manuscript Received August 14, 1990

ABSTRACT: The binding of Ca^{2+} to 4-nitro-2,1,3-benzoxadiazole (NBD)-labeled sarcoplasmic reticulum Ca^{2+}-ATPase was accelerated markedly when the pH was changed at 11 °C from 6.5 to 8.0 at the time of Ca^{2+} addition. We examined the effect of pH on the enzyme conformational transition by measuring the kinetics of NBD fluorescence rises induced by a pH jump under various ligand conditions. The fast fluorescence rise following a pH jump from 6.0 or 6.5 to various test pHs in the presence and absence of Ca^{2+} proceeded monoexponentially. The amplitude of this fluorescence rise in the presence of Ca^{2+} was independent of the test pH, whereas the observed rate constant (k_{obs}) increased markedly as the test pH increased. In contrast, the amplitude of the fast fluorescence rise in the absence of Ca^{2+} increased with increasing test pH, whereas k_{obs} decreased. MgATP or Mg^{2+} influenced the pH dependences of these parameters in a complex way except for the amplitudes measured in the presence of Ca^{2+}. These data could be simulated by using a reaction model in which Ca^{2+} binding is preceded by a rate-limiting enzyme conformational transition from a low to a high NBD fluorescence state and 1 mol each of H^+ is liberated before and after this conformational transition. MgATP or Mg^{2+} appeared to promote this conformational transition by enhancing deprotonation of the enzyme. These results suggest that deprotonation may be the primary event in the activation of the unphosphorylated enzyme by Ca^{2+}.

Activation of the sarcoplasmic reticulum calcium pump requires that 2 mol of Ca^{2+} binds to the high-affinity sites on the Ca^{2+}-ATPase (de Meis & Vianna, 1979; Martonosi & Beeler, 1983). Available kinetic evidence shows that these Ca^{2+} sites are not identical and that Ca^{2+} binding occurs in a sequential manner (Ikemoto et al., 1981; Dupont, 1982; Inesi, 1987; Petithory & Jencks, 1988a; Davidson & Berman, 1988). Several elaborate reaction models have been proposed to describe the mechanism for Ca^{2+} binding to the enzyme (Dupont, 1982; Champeil et al., 1983; Petithory & Jencks, 1988b; Fernandez et al., 1984). None of these, however, can be considered to be established because sufficient information is still not available concerning the number and the nature of the functionally important conformational states of the enzyme involved in Ca^{2+} binding as well as effects of ligands such as H^+ and Mg^{2+} on the equilibrium constant for the interconversion between these states.

It has been known for some time that binding of Ca^{2+} to the high-affinity sites of Ca^{2+}-ATPase is strongly affected by pH (Meissner, 1973; Watanabe et al., 1981). As pointed out by Tanford (1984), the following two possibilities have to be considered to account for pH effects: One is direct competition between H^+ and Ca^{2+} for the binding sites. The other is the existence of a pH-dependent equilibrium between different conformational states of the free enzyme. Hill and Inesi (1982) explained the pH dependence of their binding data on the basis of the first mechanism alone by assuming that the binding affinity changed with the extent of occupancy of the binding sites. However, the importance of the second mechanism cannot be ignored, in view of the previous reports that binding and dissociation of Ca^{2+} involve a distinct conformational change of the enzyme [see Jorgensen and Andersen (1988) for a review] and that the extent of the fluorescence change of the fluorescein-labeled enzyme induced by addition of Ca^{2+} or vanadate is highly dependent on the pH of the medium (Pick & Karlish, 1982).

Scheme I

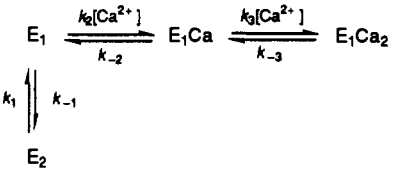

In addition to pH, it has been reported that ATP and Mg^{2+} influence the conformational transition associated with Ca^{2+} binding (Scofano et al., 1979; Inesi et al., 1980; Guillain et al., 1982; Champeil et al., 1983).

In our previous paper (Wakabayashi & Shigekawa, 1990), we analyzed the kinetics of both Ca^{2+} binding and conformational changes in the Ca^{2+}-ATPase labeled with fluorescent 7-chloro-4-nitro-2,1,3-benzoxadiazole (NBD-Cl)[1] Our data, which could be described by the mechanism illustrated in Scheme I, showed that at pH 6.5 and 11 °C, Ca^{2+} binding occurred after the conformational transition of the free enzyme from the low-fluorescent state (E_2) to the high-fluorescent state (E_1). The NBD fluorescence clearly distinguished the different conformational states of the free enzyme, because the low-fluorescence state exhibited low affinity for Ca^{2+} and intermediate affinity for ATP, whereas the high-fluorescence state exhibited high affinity for both Ca^{2+} and ATP. We further showed that ATP, by binding to a single catalytic site in E_2, accelerated the E_2 to E_1 conversion, thus increasing the overall rate of Ca^{2+} binding.

† This work was supported by Grant-in-Aid for Scientific Research on Priority Areas 62617524 from the Ministry of Education, Science and Culture of Japan.

[1] Abbreviations: NBD-Cl, 7-chloro-4-nitro-2,1,3-benzoxadiazole; EGTA, ethylene glycol bis(β-aminoethyl ether)-*N*,*N*,*N*′,*N*′-tetraacetic acid; Mes, 2-(*N*-morpholino)ethanesulfonic acid; FITC, fluorescein 5′-isothiocyanate.

0006-2960/90/0429-10613$02.50/0

In this study, we examine the effects of a pH change on Ca^{2+} binding and the conformational transition associated with it using the same NBD fluorescence signal. The present results, like our previous data (Wakabayashi & Shigekawa, 1990), provide evidence that two conformational states of the Ca^{2+}-free enzyme are involved in the Ca^{2+} binding. We further show that these two enzyme states are in a rapid, pH-dependent equilibrium, which is influenced greatly by the presence of MgATP or Mg^{2+}.

Experimental Procedures

Preparation of NBD-Labeled Ca^{2+}-ATPase. Leaky, purified Ca^{2+}-ATPase vesicles were prepared from sarcoplasmic reticulum membranes isolated from rabbit white skeletal muscle (Shigekawa et al., 1983). Modification of the Ca^{2+}-ATPase with NBD-Cl was performed as described in detail in our previous paper (Wakabayashi et al., 1990). The resulting NBD-labeled enzyme contained 7.6 ± 1.2 nmol of NBD/mg of protein (average ± SD of 13 preparations). The modified amino acid residue was Cys-344, and the predominant effect of this NBD modification was inhibition of Ca^{2+} release from the ADP-sensitive phosphoenzyme intermediate, which was responsible for the observed slow ATPase activity (5–10% of the control) (Wakabayashi et al., 1990).

Fluorescence Measurements. Equilibrium and transient kinetic fluorescence measurements were carried out at 11 °C under conditions described in the legend to each figure. Equilibrium fluorescence intensity of the NBD-enzyme was measured on a Hitachi MPF 4 spectrofluorometer with excitation at 430 nm and emission at 510 nm (Wakabayashi et al., 1990). We monitored the fluorescence kinetic transients induced by the abrupt change in the pH of the reaction medium with the aid of an Unisoku stopped-flow spectrofluorometer (FSS-300). Under the standard conditions for these experiments, syringe A contained 3 mM Mes/Tris (pH 6.0 or 6.5), 0.1 M KCl, 0.3 mM EGTA, and 0.2 mg/mL NBD-enzyme, and syringe B contained 100 mM Mes/Tris (adjusted to various pHs), 0.1 M KCl, and other ligands such as Ca^{2+}, ATP, and Mg^{2+}. Upon mixing equal volumes of these solutions, the pH of the final reaction mixture was instantly fixed at that of the solution in syringe B. For these transient kinetic measurements, the excitation light, whose wavelength (430 nm) was selected with a monochromator, was further passed through a band-path filter (Corning 5-60), and emitted light was passed through a cutoff filter (Toshiba Y-49).

Other Procedures. Time courses of $^{45}Ca^{2+}$ binding to the enzyme were measured by using a Bio-logic filtration apparatus as described previously (Wakabayashi et al., 1986). In these rapid filtration experiments, [^{3}H]glucose was included in the reaction medium to determine the filter wet volume for calculation of unbound Ca^{2+}. Determination of protein concentrations and preparation of Tris/ATP were described in the previous paper (Shigekawa et al., 1983).

Curve fitting of the experimental data was performed by an iterative least-squares method as described (Wakabayashi & Shigekawa, 1987). The best combination of values for the parameters was determined by iteration using RSS (residual sum of squares) as the best fit criterion.

Results

Effect of pH Jump on $^{45}Ca^{2+}$ Binding to NBD-Enzyme. We examined the effect of pH jump from 6.5 to 8.0 on the rate of $^{45}Ca^{2+}$ binding to the NBD-enzyme, which had been preincubated at pH 6.5 in the presence of EGTA (Figure 1). The $^{45}Ca^{2+}$ binding in 50 μM $^{45}CaCl_2$ and 5 mM $MgCl_2$ proceeded with a half-rise time of 0.37 s. This time course

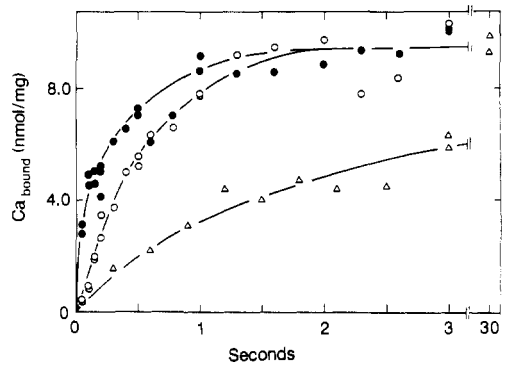

FIGURE 1: Effect of pH jump on the rate of Ca^{2+} binding to the NBD-enzyme. The NBD-enzyme (0.2 mg/mL) was preincubated with 10 mM Mes/Tris [adjusted to either pH 6.5 (△, ○) or 8.0 (●)], 0.1 M KCl, 5 mM $MgCl_2$, and 0.3 mM EGTA. $^{45}Ca^{2+}$ binding to the enzyme was then measured with a rapid filtration apparatus by washing the enzyme immobilized on the membrane filter with a solution containing 50 mM Mes/Tris [pH 6.5 (△) or 8.0 (○, ●)], 0.1 M KCl, 5 mM $MgCl_2$, 50 μM $^{45}CaCl_2$, and 10 mM [^{3}H]glucose.

was found to be markedly faster than that measured in the absence of the pH jump under otherwise the same conditions. For a comparative purpose, we also examined the effect of preincubation of the enzyme at pH 8.0 on the time course of $^{45}Ca^{2+}$ binding measured at the same pH. The $^{45}Ca^{2+}$ binding measured in the latter experiment was significantly faster than that observed following the pH jump from 6.5 to 8.0.

In our previous papers (Wakabayashi et al., 1990; Wakabayashi & Shigekawa, 1990), we presented several lines of evidence that support a reaction model in which Ca^{2+} binding to the unphosphorylated NBD-enzyme occurs following the rate-limiting conformational transition in the Ca^{2+}-free enzyme (see the introduction). The results described above thus suggest that the pH jump increases the rate of Ca^{2+} binding by accelerating the same conformational transition. In the experiments shown below, we examined the effect of pH jump on the rate of the NBD fluorescence change and its modifications by ATP and Mg^{2+}.

Effect of pH Jump on the Rate of NBD Fluorescence Rise in the Presence of Ca^{2+}. The *inset* to Figure 2 shows typical traces of the NBD fluorescence rise following pH jump from 6.5 to various test pHs in 50 μM Ca^{2+} (0.2 mM $CaCl_2$ plus 0.15 mM EGTA) and 5 mM $MgCl_2$. We found that each fluorescence rise proceeded monoexponentially to the same final level and that the first-order rate constant (k_{obs}) for the fluorescence rise increased markedly as the test pH increased. We also observed monoexponential NBD fluorescence rises when the pH jump was carried out in 50 μM Ca^{2+} alone or 50 μM Ca^{2+}, 0.3 mM ATP, and 5 mM $MgCl_2$, in place of 50 μM Ca^{2+} and 5 mM $MgCl_2$ (data not shown).

In Figure 2, we plotted estimated k_{obs} values as a function of the test pH value used. The k_{obs} value in the presence of Ca^{2+} alone exhibited the same pH dependence as that in the presence of Ca^{2+} and Mg^{2+}. In contrast, when Ca^{2+}, Mg^{2+}, and ATP were present, the k_{obs} values at each test pH were 3–13-fold greater than that obtained in the absence of ATP, with decreasing ATP stimulation being observed at higher test pH. The marked pH-dependent increase in the k_{obs} value seen in the absence of ATP agrees well with the pH jump induced acceleration of $^{45}Ca^{2+}$ binding to the enzyme described above (cf. Figure 1).

Effect of pH Jump on the Rate of NBD Fluorescence Rise in the Absence of Ca^{2+}. Next, we examined the transient kinetics of NBD fluorescence rise following pH jump in the absence of Ca^{2+} with or without 5 mM $MgCl_2$ and/or 0.3 mM ATP (Figures 3 and 4).

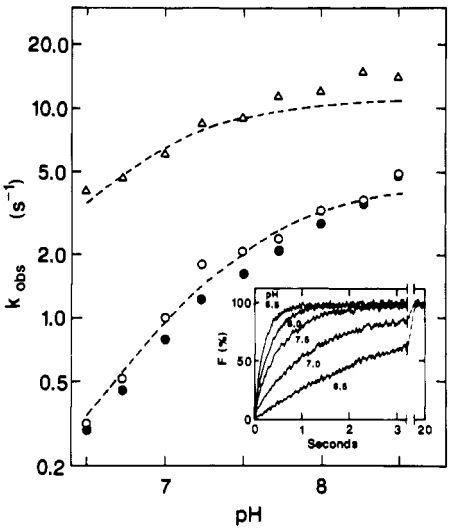

FIGURE 2: pH dependences of the k_{obs} values for the NBD fluorescence rise induced by pH jump in the presence of Ca^{2+}. The NBD-enzyme (0.2 mg/mg) in syringe A (pH 6.5) containing 0.3 mM EGTA was mixed at a 1 to 1 ratio with the medium in syringe B (adjusted to various pHs) which contained 0.4 mM $CaCl_2$ (final ionized Ca^{2+} concentration, 50 μM) and either no $MgCl_2$ and no ATP (○), 10 mM $MgCl_2$ (●), or 10 mM $MgCl_2$ plus 0.6 mM ATP (△). The k_{obs} values estimated from traces like the ones shown in the *inset* were plotted against the respective test pH used. The dashed lines were drawn according to eq A1 of the Appendix using values of parameters shown in Table I. The *inset* shows typical traces for the pH jump induced NBD fluorescence rise obtained in 50 μM Ca^{2+} and 5 mM Mg^{2+}.

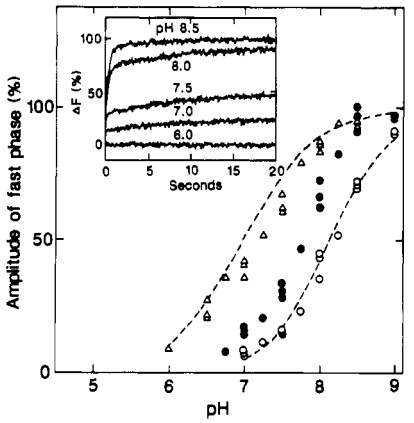

FIGURE 3: pH dependences of the amplitude of the fast phase of the NBD fluorescence rise following pH jump in the absence of Ca^{2+}. The NBD-enzyme (0.2 mg/mL) in syringe A (pH 6.0) containing 0.3 mM EGTA was mixed at a 1 to 1 ratio with the medium in syringe B (adjusted to various pHs) which contained 0.3 mM EGTA and either no $MgCl_2$ and no ATP (○), 10 mM $MgCl_2$ (●), or 10 mM $MgCl_2$ plus 0.6 mM ATP (△), and then time courses for the fluorescence rise were followed as described under Experimental Procedures. The amplitudes of the fast phase of fluorescence rise measured under various ligand conditions were plotted against the test pH values used. The dashed lines were drawn according to eq A4 of the Appendix using values of parameters listed in Table I. The *inset* shows the typical traces for the fluorescence rise obtained in the presence of 5 mM $MgCl_2$ at the indicated test pH.

The *inset* to Figure 3 shows records for the NBD fluorescence rise induced by pH jump from 6.0 to various test pHs in the presence of 5 mM $MgCl_2$. In the absence of Ca^{2+}, the fluorescence rise consisted of two kinetic components: an initial fast phase and a late, slow one. The amplitude of the initial fast component increased with increasing test pH values. In contrast, the slow component, which had a half-rise time of about 7 s, was most evident when the test pH was in the intermediate range (~7.5). When the same type of experiments were repeated in the presence of ATP and Mg^{2+} or in the absence of both ATP and Mg^{2+}, similar biphasic time courses of the NBD fluorescence rise were obtained (data not shown).

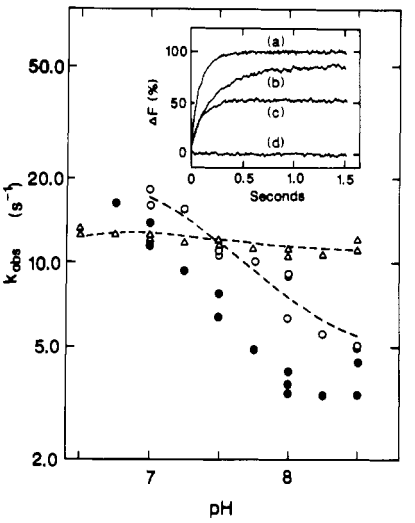

FIGURE 4: pH dependences of the k_{obs} values for the fast phase of the NBD fluorescence rise induced by pH jump in the absence of Ca^{2+}. The NBD-enzyme (0.2 mg/mL) in syringe A (pH 6.5) containing 0.3 mM EGTA was mixed at a 1 to 1 ratio with the medium in syringe B (adjusted to various pHs) which contained 0.3 mM EGTA and either no $MgCl_2$ and no ATP (○), 10 mM $MgCl_2$ (●), or 10 mM $MgCl_2$ plus 0.6 mM ATP (△). The k_{obs} values for the fast phase of the NBD fluorescence rise measured under various ligand conditions were plotted against the respective test pH used. The dashed lines were drawn according to eq A1–A3 of the Appendix using values of parameters listed in Table I. The *inset* shows typical traces for the fast phase of the NBD fluorescence rise induced by the pH jump from 6.5 to 8.0 in the presence of 0.3 mM EGTA and under the following conditions: (a) 5 mM $MgCl_2$ and 0.3 mM ATP; (b) 5 mM $MgCl_2$; (c) with no additional ligand; (d) no pH jump.

In Figure 3, we plotted the amplitudes of the fast NBD fluorescence rise measured under various ligand conditions as a function of the final test pH of the medium. We found that ATP or Mg^{2+} shifted the pH dependence of the amplitude of the fast fluorescence rise toward the acidic side relative to that obtained in the absence of ATP and Mg^{2+}, without influencing the maximal amplitude. The pH shift was greater with 0.3 mM ATP and 5 mM $MgCl_2$ than with 5 mM $MgCl_2$.

The *inset* to Figure 4 shows records for the initial phase of the NBD fluorescence rise following the pH jump from 6.5 to 8 in the absence of Ca^{2+} and under different ligand conditions. As typically shown in these records, the initial fast fluorescence rise was always monoexponential, although its amplitude and its k_{obs} value differed significantly depending on the ligand present at the time of the pH change. We found that in the absence of Ca^{2+}, the k_{obs} value was a complex function of the test pH value used (Figure 4). The k_{obs} value measured in the absence of ATP and Mg^{2+} decreased as the test pH increased. Mg^{2+} at 5 mM enhanced this inhibitory effect of the high test pH, whereas 0.3 mM ATP abolished it.

In Figure 5, we calculated the ratio between the k_{obs} value for the NBD fluorescence rise measured at a given test pH in the presence of 50 μM Ca^{2+} (Figure 2) and the k_{obs} value for the fast fluorescence rise measured at the same test pH but in the absence of Ca^{2+} (Figure 4). We plotted the value for this ratio obtained under each ligand condition as a function of the test pH used. It is important to note that except for the data at pH >8, the observed pH dependences are very similar to those seen in Figure 3, where the amplitude of the fast NBD fluorescence rise in the absence of Ca^{2+} was plotted as a function of the test pH. The agreement in these pH

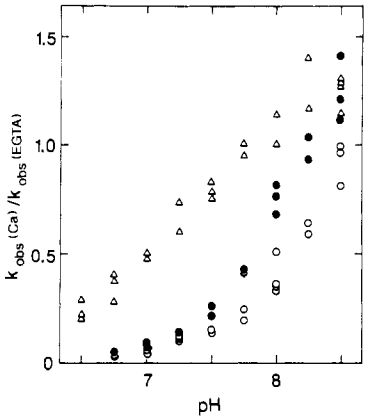

FIGURE 5: pH dependences of the ratios between the k_{obs} values for the fast NBD fluorescence rise measured in the presence and absence of Ca^{2+} under various ligand conditions. The k_{obs} values for the pH-induced NBD fluorescence rise either in 50 μM Ca^{2+} or in 0.3 mM EGTA were measured as described in the legends to Figures 2 and 4, respectively. The calculated ratios between these k_{obs} values measured in the presence of no $MgCl_2$ and no ATP (○), 5 mM $MgCl_2$ (●), or 0.3 mM ATP and 5 mM $MgCl_2$ (△) were plotted against the respective test pH used. The data shown in this figure were the combined results from three experiments with different preparations of the NBD-enzyme.

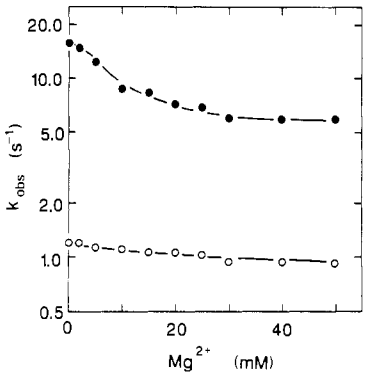

FIGURE 6: Effect of the Mg^{2+} concentration on the k_{obs} value for the NBD fluorescence rise measured in the presence or absence of Ca^{2+}. The NBD-enzyme in syringe A (pH 6.5) containing 0.3 mM EGTA was mixed at a 1 to 1 ratio with the medium in syringe B (adjusted to pH 7.0) which contained various concentrations of $MgCl_2$ and either 1.3 mM $CaCl_2$ (○) or 0.3 mM EGTA (●), and then time courses for the fluorescence rise were measured at pH 7.0 as described under Experimental Procedures. In the absence of Ca^{2+}, the k_{obs} was calculated from the fast phase of the fluorescence rise (cf. *inset* to Figure 4).

dependences strongly suggests that the high-fluorescence species of the Ca^{2+}-free enzyme, whose existence was detected in the above pH jump experiments (Figures 3 and 4), is kinetically qualified as being an intermediate for Ca^{2+} binding to the enzyme (see Discussion).

Effect of Mg^{2+} Concentration on the k_{obs} Value for NBD Fluorescence Rise. We measured the Mg^{2+} concentration dependence of the k_{obs} value for the NBD fluoresence rise following the pH jump from 6.5 to 7.0 in the presence or absence of Ca^{2+} (Figure 6). In the absence of Ca^{2+}, high Mg^{2+} decreased the k_{obs} value for the fluorescence rise by up to 65%, with about 10 mM $MgCl_2$ producing an apparent half-maximal inhibition. In the presence of 0.5 mM Ca^{2+}, however, added Mg^{2+} decreased the k_{obs} value only slightly.

pH Dependence of Equilibrium NBD Fluorescence Levels. Figure 7 shows equilibrium levels of the NBD fluorescence measured at different pHs in the presence of EGTA and under various ligand conditions. The figure also shows the equilibrium fluorescence levels measured in the presence of 0.5 mM vanadate or $CaCl_2$. In the presence of EGTA (absence of Ca^{2+}

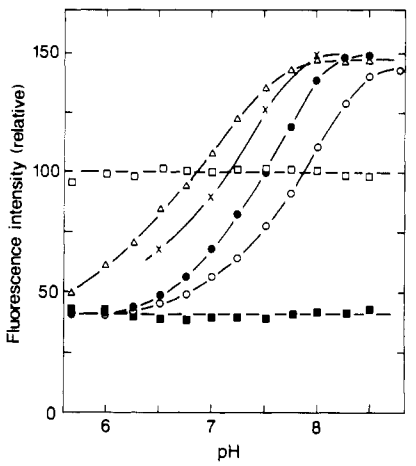

FIGURE 7: pH dependences of the equilibrium level of NBD fluorescence measured under various ligand conditions. Equilibrium levels of the NBD fluorescence were measured with 0.1 mg/mL NBD-enzyme at 11 °C in 50 mM Mes/Tris (adjusted to various pHs), 0.1 M KCl, 0.3 mM EGTA, and 5 mM $MgCl_2$ in the presence of the following additional ligands: (■) 0.5 mM vanadate; (□) 0.5 mM $CaCl_2$; (△) 0.3 mM ATP; (●) no addition. Open circles show the result of an experiment in which $MgCl_2$ was omitted from the reaction mixture. Crosses represent the fluorescence intensity at infinite Mg^{2+} concentration, which was estimated at each pH as described in the text.

or vanadate), the fluorescence level was markedly dependent on the medium pH, and its pH dependence was influenced greatly by the presence of ATP and/or Mg^{2+}. In the absence of these ligands, the fluorescence level, which at acidic pH (6.0–6.5) was almost equal to that obtained in the presence of vanadate, increased with increasing pH, reaching the maximum at about pH 8.5. This pH dependence could be fitted approximately to a titration curve was a pK value of 7.8.

ATP at 0.3 mM (plus 5 mM $MgCl_2$) shifted the pH dependence of the equilibrium NBD fluorescence level by about 1 pH unit toward the acidic side without influencing both the minimum and the maximum (Figure 7). The extent of this shift was similar (about 1 pH unit) when the ATP concentration was raised from 0.3 to 1.0 mM in the presence of either 1 or 5 mM $MgCl_2$.

In the presence of 5 mM $MgCl_2$ alone, the pH curve was complex; Mg^{2+} exerted a more pronounced effect at alkaline pH than at acidic pH. This seemingly uneven effect of 5 mM $MgCl_2$, was due probably to the pH-dependent change in the affinity of the enzyme for Mg^{2+}. In fact, when the NBD fluorescence intensity at infinite Mg^{2+} concentration, which was estimated at each pH from the linear double-reciprocal plot of the observed fluorescence level versus the added Mg^{2+} concentration, was plotted against pH, the pH dependence could be fitted approximately to a titration curve with a pK value of 7.1 [Figure 7 (×)]. From the double-reciprocal plot of the fluorescence level versus the Mg^{2+} concentration at pH 7.0, we obtained a value of 11 mM for the affinity of the enzyme for Mg^{2+} at pH 7.0. This value agrees well with the concentration of Mg^{2+} (10 mM) at which we observed a half-maximal decrease of the k_{obs} value for the NBD-fluorescence rise following the pH jump from 6.5 to 7.0 in the absence of Ca^{2+} (Figure 6).

We found that the fluorescence level in the presence of 0.5 mM Ca^{2+} or vanadate was independent of the pH of the medium (Figure 7). These fluorescence levels were also insensitive to changes in temperature and the concentration of KCl (from 0 to 100 mM) (data not shown). It is interesting to note that the maximum level of equilibrium fluorescence seen in the presence of EGTA at pH 8.5 and 5 mM $MgCl_2$

was 1.3 ± 0.1 (average ± SD for seven preparations) times as high as the level for the enzyme with bound calcium. The fluorescence level for the latter was about 2 times as high as that seen in the presence of vanadate (Wakabayashi et al., 1990; see also Figure 7).

In the presence of EGTA, the pH curve for the equilibrium fluorescence level (Figure 7) was similar to the corresponding pH curve for the amplitude of the pH jump induced fast NBD fluorescence rise (Figure 3) except that the former was shifted by about 0.3 pH unit toward the acidic side relative to the latter. We found that the maximum pH-dependent increase obtained in the equilibrium fluorescence measurement was the same as the maximum amplitude of the pH jump induced fast fluorescence rise. This finding indicates that the maximum amplitude of the fast fluorescence rise exceeds the fluorescence level for the enzyme with bound calcium.

Discussion

pH-Induced Acceleration of Enzyme Conformational Change. The present results show that pH jump accelerates markedly the binding of Ca^{2+} and the NBD fluorescence rise associated with it (Figures 1 and 2). In addition, preincubation of the enzyme at high pH (8.0) caused much faster Ca^{2+} binding than that seen following pH jump from 6.5 to the same high pH (Figure 1). These results suggest that pH jump increases the rate of Ca^{2+} binding by accelerating the enzyme conformational change. As discussed briefly in the introduction, the reaction model shown in Scheme I successfully described the kinetics of Ca^{2+} binding and NBD fluorescence change at pH 6.5 and 11 °C in the presence and absence of ATP (Wakabayashi & Shigekawa, 1990). ATP was shown to increase the rate of Ca^{2+} binding to the NBD-enzyme by accelerating the rate-limiting conformational transition in the Ca^{2+}-free enzyme from a low-fluorescence state to a high-fluorescence state. Thus, an intriguing question would be whether the pH jump accelerates the Ca^{2+} binding in a similar mechanism.

In the Ca^{2+}-free NBD-enzyme, pH jump from 6.0 to various test pHs induced fast NBD fluorescence rises, followed by very slow ones (*inset* to Figure 3). The slow phase was too slow for it to be involved directly in Ca^{2+} binding. Interestingly, the slow phase almost disappeared at high test pH (~8.5), where the amplitude of the initial fast phase reached the maximum (cf. Figure 3). We therefore speculate that two enzyme species, whose formations were monitored by the slow and fast fluorescence rises, might have the same fluorescence intensity and that the slow species might be derived from the fast species in a slow side reaction.

The fast fluorescence phase, on the other hand, was sufficiently rapid to account for the time course of Ca^{2+} binding (cf. Figures 1 and 4). It was monoexponential under various ligand conditions (Figure 4), and its amplitude became larger as the size of the pH jump increased (*inset* to Figure 3). The observed pH dependences of the amplitude of the fast phase are similar to those obtained for the equilibrium levels of NBD fluorescence measured at different pHs (Figure 7), except that the latter curves are shifted by about 0.3 pH unit toward the acidic side (compare Figures 3 and 7). We can provide an explanation for this small pH shift, assuming that the slow phase is derived from the fast phase (see above); only under the equilibrium conditions, the slow phase could contribute to the total fluorescence rise, which would shift the pH curves for the equilibrium fluorescence signal toward the acidic side relative to those for the amplitude of the fast phase. Exactly the same type of explanation was provided previously (Wakabayashi & Shigekawa, 1990) for the observed difference between the ATP concentration dependences of the equilibrium fluorescence increase and the amplitude of the ATP-induced fast fluorescence rise. Thus, the results obtained both in the transient kinetic and in the equilibrium measurements indicate that the Ca^{2+}-free NBD-labeled enzyme is in a rapid, pH-dependent equilibrium between low- and high-fluorescence states and that high pH stabilizes the latter.

The kinetics of rapid conversion between these enzyme states in the presence and absence of Ca^{2+} and their modifications by ATP and Mg^{2+} (Figures 2 and 4) could be described by the model in Scheme I, assuming that the low- and high-fluorescence states correspond to E_2 and E_1 of Scheme I. This assumption allowed us to estimate the size of the fraction of the Ca^{2+}-free enzyme that was present in the form of E_1 after the rapid pH equilibration, by calculating the ratio between the k_{obs} value for the pH jump induced fast-fluorescence rise in 50 μM Ca^{2+} (Figure 2) and the corresponding k_{obs} value in the absence of Ca^{2+} (Figure 4). This is because in Scheme I, the k_{obs} value measured in a saturating concentration of Ca^{2+} would give an estimate of the value for the forward rate constant k_1, whereas that measured in the absence of Ca^{2+} would represent the sum of the rate constants k_1 and k_{-1} for the forward and reverse reactions, respectively. We plotted the values for the calculated ratio as a function of the test pH used (Figure 5). We found that at least for the test pHs below 8.0, they exhibited almost identical pH dependences with those for the amplitude of the fast NBD fluorescence rise measured in the absence of Ca^{2+} (compare Figures 3 and 5).

It should be noted that the values for the ratio described above slightly exceed 1 at high test pH (Figure 5). This could be due to our overestimation of the k_1 value because we found previously (Wakabayashi & Shigekawa, 1990) that a new faster pathway for the NBD fluorescence rise became available when Ca^{2+} bound to the low-affinity site on the enzyme. At pH 8.0–8.5, 50 μM Ca^{2+} would be high enough to activate the low-affinity pathway at least partly, which could result in acceleration of the NBD fluorescence rise.

The data discussed above therefore strongly support a view that the pH jump, like ATP addition, increases the rate of Ca^{2+} binding by accelerating the conformational transition in the Ca^{2+}-free enzyme, which is a true step of the Ca^{2+} binding reaction.

Figure 2 shows the pH dependences of the rate constant k_1 for the forward reaction of the transition from the low- (E_2) to high-fluorescence (E_1) states as defined in Scheme I. The k_1 values increased markedly as the test pH increased. On the other hand, Figure 8 shows the pH dependences of the reverse rate constant (k_{-1}) for the same E_2 to E_1 transition. The k_{-1} values were estimated by subtracting the k_{obs} values measured in the presence of Ca^{2+} (Figure 2) from the corresponding values obtained in the absence of Ca^{2+} (Figure 4). The k_{-1} values became very low as the test pH approached ~8.5 (Figure 8). We consider that the negative k_{-1} values at high test pH were caused by overestimation of the k_1 values due to activation of the low-affinity pathway (see above). These data thus suggest that at high pH (~8.5), the equilibrium between the E_1 and E_2 states of the Ca^{2+}-free enzyme is shifted almost completely to the E_1 state.

There are two other findings that need comments. First, the NBD fluorescence rise in the presence of Ca^{2+} was always monoexponential, whereas that in the absence of Ca^{2+} was biphasic (Figures 2 and 3). We interpret these finding as indicating that Ca^{2+} reacts rapidly with the initial, fast component of the NBD fluorescence rise (E_1) and depletes it, thus preventing the formation of the slow component from it.

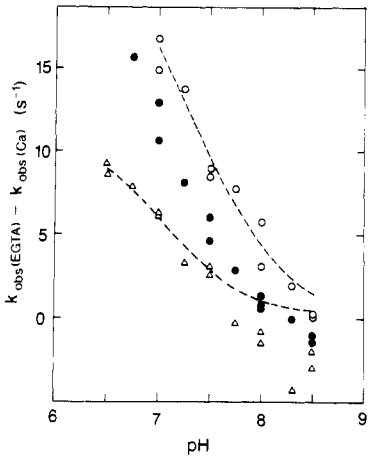

FIGURE 8: pH dependences of calculated values for the rate constant for the reverse reaction (k_{-1}) of the E_2 to E_1 transition. The values for k_{-1} were estimated by subtracting the k_{obs} values measured at the respective test pH in the presence of Ca^{2+} (Figure 2) from the corresponding k_{obs} values obtained in the absence of Ca^{2+} (Figure 4). The k_{obs} values were measured in the presence of no $MgCl_2$ and no ATP (○), 5 mM $MgCl_2$ (●), or 0.3 mM ATP and 5 mM $MgCl_2$ (△).

Second, the high-fluorescence state (E_1) exhibited a fluorescence level about 1.3-fold that for the enzyme with bound calcium and about 2.6-fold that for the low-fluorescence state (see Figure 7 and Results). We (Wakabayashi et al., 1990) previously found that at pH 6.0 and 11 °C, the NBD-enzyme was grouped into two states, one being a higher fluorescence state with bound calcium (the unphosphorylated enzyme with bound calcium, the enzyme–ATP–calcium complex, and the ADP-sensitive phosphoenzyme) and the other being a lower fluorescence state without bound calcium (the unphosphorylated enzyme without bound calcium, the ADP-insensitive phosphoenzyme, and the enzyme–vanadate complex). The enzyme state with even higher NBD fluorescence detected in these pH jump experiments clearly is the third state of the enzyme. This high-fluorescence state (E_1) seems to appear transiently during Ca^{2+} binding to the unphosphorylated enzyme. If this interpretation is correct, a very fast drop in the NBD fluorescence should have occurred somewhere before the formation of the Ca^{2+}-bound enzyme (E_1Ca_2) (cf. Scheme I), because the overall NBD fluorescence rise induced by the pH jump in the presence of Ca^{2+} was simply monoexponential (*inset* to Figure 2). In this connection, it should be pointed out that introduction of a difference in the fluorescence levels for E_1 and E_1Ca_2 does not affect the results of simulations of the NBD fluorescence data presented in our previous paper (Wakabayashi & Shigekawa, 1990), as long as we assume that the fluorescence drops upon formation of E_1Ca (cf. Scheme I).

Mechanism for H^+ Participation in the Conformational Transition. The amplitude of the pH-induced, fast NBD fluorescence rise measured in the Ca^{2+}-deprived enzyme displayed a pH titration curve involving an apparent pK value of about 8 in the absence of ATP and Mg^{2+} (Figure 3). ATP at 0.3 mM shifted this pH curve by 1 pH unit toward the acidic side (Figure 3). This shift was actually affected by the MgATP complex under the conditions used. Metal-free ATP was also effective, but its maximal effect and its apparent affinity were about half of those for MgATP.[2] Mg^{2+} also exerted a similar but weaker effect (Figures 3 and 7). It is important to note that at neutral or acidic pH, the MgATP- or Mg^{2+}-induced transition from the low- to high-fluorescence

[2] S. Wakabayashi and M. Shigekawa, unpublished observation.

Scheme II

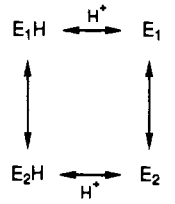

Table I: Values of Kinetic Parameters for Scheme III[a]

parameters	no addition	plus ATP
k_{+c} (s^{-1})	4.4 ± 0.1[b]	11 ± 1
k_{-c} (s^{-1})	23 ± 3	12 ± 1
pK_{H1}	7.4 ± 0.1	7.0 ± 0.1
pK_{H2}	7.6 ± 0.0	6.8 ± 0.1

[a] Parameters are defined in Scheme III. The parameter values shown in this table were obtained by iterative nonlinear least-squares fits of the data shown in Figures 2 and 8 by using eqs A1 and A2 of the Appendix. The curve fitting for the ATP series (presence of 0.3 mM ATP and 5 mM $MgCl_2$) was performed by using the data obtained at pH below 7.75 to avoid the extra effect of high test pH (see text). [b] Standard error of the estimate.

states was incomplete even when a saturating concentration of each ligand was present in the reaction medium (see Figure 7 and Results). These findings suggest that the equilibrium between the high- and low-fluorescence states of the enzyme is primarily determined by the extent to which the enzyme was protonated and that ATP or Mg^{2+} plays only a modulatory role in this enzyme–proton interaction.

As discussed above, the kinetics of the fast fluorescence rise induced by the pH jump could be fitted to the model in Scheme I. The values for the apparent rate constants k_1 and k_{-1} were highly pH sensitive (Figures 2 and 8). The complex pH dependences of these rate constants and of the amplitude of the fast fluorescence rise (Figure 3) could not be fitted to a simple model such as the one shown in Scheme II, in which only one proton was involved in the conformational transition. Scheme II was used by Pick and Karlish (1982) to explain the kinetics of the pH-induced fluorescence change in the fluorescein-labeled free enzyme.

Our data could be fitted to Scheme III in which two protons were involved in the conformational transition and where K_{H1} and K_{H2} are proton dissociation constants of E_1H and E_2H_2, respectively, and K_c is the conformational equilibrium constant. In this scheme, we assume that dissociation and association of protons with the enzyme are rapid as compared to the rates of the conformational transition and that each mole of H^+ is liberated before and after the conformational transition of the enzyme. This model can readily explain the well-documented competition between Ca^{2+} ions and protons for the Ca^{2+} binding sites of the free enzyme (Meissner, 1973; Watanabe et al., 1981; Guilllain et al., 1982), if Ca^{2+} at micromolar concentrations binds only to the deprotonated form of the E_1 state.

Scheme III

$$E_2H_2 \overset{H^+}{\leftrightarrow} E_2H \underset{k_{-c}}{\overset{k_{+c}}{\rightleftharpoons}} E_1H \overset{H^+}{\leftrightarrow} E_1$$
$$K_{H2} \qquad K_c \qquad K_{H1}$$

Scheme III and values of parameters listed in Table I reproduced the complex pH dependences of the NBD fluorescence data obtained either in the presence of MgATP or in the absence of ATP and Mg^{2+} (dashed line in Figures 2, 3, 4, and 8). We did not simulate the data obtained in the presence of Mg^{2+} alone because of the pH effect on the affinity

of the enzyme for Mg^{2+} (see Figure 7 and Results). On the basis of these satisfactory simulations, we propose that in the absence of ATP and Mg^{2+}, the enzyme is in the form of E_2H_2 at acidic pH (6–6.5) whereas it is in the form of E_1 at alkaline pH (~8.5). This proposal is consistent with our previous assumption that the enzyme is mostly in the low-fluorescence (E_2) state under the standard conditions of our previous study [pH 6.5, 11 °C, low Mg^{2+} concentration (2 mM), no Ca^{2+}] (Wakabayashi & Shigekawa, 1990).

According to Table I, 0.3 mM ATP increased the forward rate constant (k_{+c}) of the E_2H to E_1H transition by 2.5-fold and decreased the reverse rate constant (k_{-c}) of the same transition to a similar extent. In addition, it increased the proton dissociation constants K_{H1} and K_{H2} from $10^{-7.4}$ to $10^{-7.0}$ and from $10^{-7.6}$ to $10^{-6.8}$, respectively. Thus, it seems that ATP influences both the conformational equilibrium constant (K_c) and the proton dissociation constants.

Mg^{2+}, on the other hand, did not exert a significant effect on the pH dependence of the forward rate constant (k_1) for the E_2 to E_1 transition in Scheme I (Figures 2 and 6). Instead, Mg^{2+} at millimolar concentrations ($K_{1/2}$, ~10 mM) reduced the apparent rate constant (k_{-1}) for the reverse reaction of the same conformational transition (Figures 6 and 8). These results suggest that Mg^{2+}, by interacting with the E_1 state of the enzyme, either increases the proton dissociation constant (K_{H1}) of the E_1 state or decreases the rate constant (k_{-c}) for the reverse reaction of the E_2H to E_1H transition, or both. This effect of Mg^{2+}, which stabilizes the high-fluorescent state (E_1 state) (Figures 3 and 7), is consistent with the observations by other workers (Guillain et al., 1982; Loomis et al., 1982; Champeil et al., 1985) that high Mg^{2+} stabilizes a form of the free enzyme unfit for phosphorylation by P_i.

These NBD fluorescence data indicate that dissociation and association of protons are intimately involved in the enzyme conformational transition. It is important to measure directly the movements of protons and to compare them with the movements of Ca^{2+} ions and the kinetics of pH-dependent NBD fluorescence changes. Previously, Chiesi and Inesi (1980) measured the amount of H^+ liberated following addition of Ca^{2+} to native sarcoplasmic vesicles at pH 6.0. They found that the ratio of Ca^{2+} bound to H^+ liberated was about 1. We also obtained a similar 1 H^+/1 Ca^{2+} stoichiometry with the NBD-enzyme at pH 6.5 and 5 mM Mg^{2+} under conditions similar to those used here.[2] We also found that the kinetics of H^+ liberation were similar to those of the Ca^{2+}-induced NBD fluorescence rise.[2] Although these findings are consistent with our model in Scheme III, we at present have no information as to the nature and locations of the H^+-liberating sites on the enzyme and how many protons are actually bound and released in the overall process of binding of Ca^{2+} to the enzyme. In addition, we have no information on the mechanism linking H^+ liberation to the induction of the change in the enzyme conformation.

An intriguing question related to the model in Scheme III is whether the H^+ liberation detected could be a part of the mechanism involved in countertransport of protons for transport of Ca^{2+} ions. Yamaguchi and Kanazawa (1985) reported that during ATP hydrolysis by the leaky, purified ATPase, protons were taken up when the phosphorylated enzyme accumulated, whereas an almost equivalent amount of H^+ was liberated when Ca^{2+} bound to the unphosphorylated form of the enzyme. Other studies (Wakabayashi & Shigekawa, 1987; Bishop & Al-Shawi, 1988; Yamaguchi & Kanzawa, 1988) also showed that high pH inhibits hydrolysis of the ADP-insensitive phosphoenzyme, suggesting that uptake of protons by this form of phosphoenzyme on the lumenal side of the membrane may be required for its hydrolysis. Although these and other (Madeira, 1978; Kodama et al., 1980; Chiesi & Inesi, 1980) results support the idea of countertransport of protons, further information about the movements of protons and Ca^{2+} ions in relation to the enzyme conformational change both in the phosphorylated and in the unphosphorylated enzyme intermediates is needed to clarify the question of the Ca^{2+}–H^+ antiport.

Appendix

Assuming rapid dissociation and association of protons with the enzyme, Scheme III can be reduced to the following form:

$$e_2 \underset{k_{-1}}{\overset{k_1}{\rightleftharpoons}} e_1$$

where

$$[e_1] = [E_1] + [E_1H]$$

$$[e_2] = [E_2H] + [E_2H_2]$$

$$k_1 = k_{+c}\frac{1}{1 + [H]/K_{H2}} \quad \text{(A1)}$$

$$k_{-1} = k_{-c}\frac{[H]/K_{H1}}{1 + [H]/K_{H1}} \quad \text{(A2)}$$

The observed rate constant (k_{obs}) for the fast phase of the pH jump induced fluorescence rise in the absence of Ca^{2+} is given by

$$k_{obs} = k_1 + k_{-1} \quad \text{(A3)}$$

On the other hand, the fractional amount of e_1 (F) after the pH jump is given by the equation:

$$F = \frac{1 + [H]/K_{H1}}{1 + (1 + K_c)[H]/K_{H1} + K_c[H]^2/K_{H1}K_{H2}} \quad \text{(A4)}$$

where K_c is k_{-c}/k_{+c}.

Registry No. ATPase, 9000-83-3; Ca, 7440-70-2; MgATP, 1476-84-2; Mg, 7439-95-4.

References

Bishop, J. E., & Al-Shawi, M. K. (1988) *J. Biol. Chem. 263*, 1886–1892.

Champeil, P., Gingold, M. P., & Guillain, F. (1983) *J. Biol. Chem. 258*, 4453–4458.

Champeil, P., Guillain, F., Venien, C., & Gingold, M. P. (1985) *Biochemistry 24*, 69–81.

Chiesi, M., & Inesi, G. (1980) *Biochemistry 19*, 2912–2918.

Davidson, G. A., & Berman, M. C. (1988) *J. Biol. Chem. 263*, 11786–11791.

de Meis, L., & Vianna, A. L. (1979) *Annu. Rev. Biochem. 48*, 275–292.

Dupont, Y. (1982) *Biochim. Biophys. Acta 688*, 75–87.

Fernandez-Belda, F., Kurzmack, M., & Inesi, G. (1984) *J. Biol. Chem. 259*, 9687–9698.

Guillain, F., Gingold, M. P., & Champeil, P. (1982) *J. Biol. Chem. 257*, 7366–7371.

Hill, T. L., & Inesi, G. (1982) *Proc. Natl. Acad. Sci. U.S.A. 79*, 3978–3982.

Ikemoto, N., Garcia, A. M., Kurobe, Y., & Scott, T. L. (1981) *J. Biol. Chem. 256*, 8593–8601.

Inesi, G. (1987) *J. Biol. Chem. 262*, 16338–16342.

Insei, G., Kurzmack, M., Coan, C., & Lewis, D. E. (1980) *J. Biol. Chem. 255*, 3025–3031.

Jorgensen, P. L., & Andersen, J. P. (1988) *J. Membr. Biol. 103*, 95–120.

Kodama, T., Kurebayashi, N., & Ogawa, Y. (1980) *J. Biochem. (Tokyo) 88*, 1259-1265.
Loomis, C. R., Martin, D. W., McCaslin, D. R., & Tanford, C. (1982) *Biochemistry 21*, 151-156.
Madeira, V. M. C. (1978) *Arch. Biochem. Biophys. 185*, 316-325.
Martonosi, A., & Beeler, T. J. (1983) *Handb. Physiol. 10*, S417-S485.
Meissner, G. (1973) *Biochim. Biophys. Acta 298*, 906-926.
Petithory, J. R., & Jencks, W. P. (1988a) *Biochemistry 27*, 5553-5564.
Petithory, J. R., & Jencks, W. P. (1988b) *Biochemistry 27*, 8626-8635.
Pick, U., & Karlish, S. J. D. (1982) *J. Biol. Chem. 257*, 6120-6126.
Scofano, H. M., Vieyra, A., & de Meis, L. (1979) *J. Biol. Chem. 254*, 10227-10231.
Shigekawa, M., Wakabayashi, S., & Nakamura, H. (1983) *J. Biol. Chem. 258*, 8698-8707.
Tanford, C. (1984) *CRC Crit. Rev. Biochem. 17*, 123-151.
Wakabayashi, S., & Shigekawa, M. (1987) *J. Biol. Chem. 262*, 9121-9129.
Wakabayashi, S., & Shigekawa, M. (1990) *Biochemistry 29*, 7309-7318.
Wakabayashi, S., Ogurusu, T., & Shigekawa, M. (1986) *J. Biol. Chem. 261*, 9762-9769.
Wakabayashi, S., Imagawa, T., & Shigekawa, M. (1990) *J. Biochem. (Tokyo) 107*, 563-571.
Watanabe, T., Lewis, D., Nakamoto, R. Kurzmack, M., Fronticelli, C., & Inesi, G. (1981) *Biochemistry 20*, 6617-6625.
Yamaguchi, M., & Kanazawa, T. (1985) *J. Biol. Chem. 260*, 4896-4900.
Yamaguchi, M., & Kanazawa, T. (1988) in *Energy Transduction in ATPases* (Mukohata, Y., Morales, M., & Fleischer, S. Eds.) pp 274-281, Yamada Science Foundation, Osaka.

Purification to Homogeneity of Latent and Active 58-Kilodalton Forms of Human Neutrophil Collagenase†

Kasim A. Mookhtiar and Harold E. Van Wart*
Department of Chemistry and Institute of Molecular Biophysics, Florida State University, Tallahassee, Florida 32306
Received June 6, 1990; Revised Manuscript Received August 9, 1990

ABSTRACT: Latent and active 58-kDa forms of human neutrophil collagenase (HNC) have been purified to homogeneity. Buffy coats were extracted in the presence and absence of phenylmethanesulfonyl fluoride to generate crude starting preparations that contained latent and active HNC, respectively. The buffers used in preparing these extracts and for all subsequent chromatographic steps contained NaCl at a concentration of 0.5 M or greater, 0.05% Brij-35, concentrations of $CaCl_2$ of 5 mM or greater, and (when feasible) 50 μM $ZnSO_4$ to stabilize the HNC. The collagenase activity in the buffy coat extracts was adsorbed to a Reactive Red 120-agarose column at pH 7.5 in 0.5 M NaCl and was eluted when the NaCl concentration was increased to 1 M. The active and *p*-(chloromercuri)benzoate-activated latent enzymes were next adsorbed to a Sepharose-CH-Pro-Leu-Gly-NHOH affinity resin in 1 M NaCl at pH 7.5 and desorbed at pH 9 to give a fraction containing only HNC and a small amount of neutrophil gelatinase. The latter enzyme was removed by passage over a gelatin-Sepharose column in 1 M NaCl at pH 7.5. The purified samples of active and latent HNC were obtained with typical cumulative yields of 32 and 82% and specific activities toward soluble rat type I collagen at 30 °C of 7200 and 12000 μg min^{-1} mg^{-1}, respectively. These specific activities are markedly higher than previously reported for HNC. Both active and latent HNC exhibit a single band on sodium dodecyl sulfate-polyacrylamide gel electrophoresis both in the presence and in the absence of 2-mercaptoethanol. The mobility of latent HNC is consistent with a molecular weight of approximately 58K, with the active form exhibiting a slightly lower (<1-2K) molecular weight.

The breakdown of interstitial collagens in all higher organisms is believed to be initiated by specific collagenases (EC 3.4.24.7) (Birkedal-Hansen, 1987; Van Wart & Mookhtiar, 1990). The key feature of these enzymes is their ability to hydrolyze the triple-helical collagen monomers of collagen fibrils at a specific locus to produce characteristic three-fourths and one-fourth fragments. Because of their involvement in both normal and pathological connective tissue catabolism, it is vital that the collagenases produced by different human cells be isolated and characterized in detail. The most intensively studied human collagenase is that originally isolated from skin fibroblast cultures (Stricklin et al., 1977). Human fibroblast collagenase (HFC)[1] is a metalloproteinase that is produced only by de novo synthesis and secreted into the extracellular space as a zymogen. The sequence of the secreted zymogen, which has a molecular weight of 52K, has been

† This work was supported by Research Grant GM27939 from the National Institutes of Health.
* Author to whom correspondence should be addressed at the Institute of Molecular Biophysics, Florida State University.

[1] Abbreviations: HNC, human neutrophil collagenase; HFC, human fibroblast collagenase; HNG, human neutrophil gelatinase (type IV collagenase); SDS-PAGE, sodium dodecyl sulfate-polyacrylamide gel electrophoresis; Tricine, *N*-[tris(hydroxymethyl)methyl]glycine; Mes, 2-(*N*-morpholino)ethanesulfonic acid; Tris, tris(hydroxymethyl)aminomethane; Brij-35, polyoxyethylene(23) lauryl ether; PCMB, *p*-(chloromercuri)benzoate; PMSF, phenylmethanesulfonyl fluoride.

0006-2960/90/0429-10620$02.50/0